International Journal of Computer Information Systems and Industrial Management Applications.
ISSN 2150-7988 Volume 6 (2014) pp. 126 - 138

Finger Nail Plate: A New Biometric Identifier

Shruti Garg, Amioy Kumar, and M. Hanmandlu

Biometrics Research Laboratory
Department of Electrical Engineering,
Indian Institute of Technology Delhi,
New Delhi, India
shrutigarg29@gmail.com, amioy.iitd@gmail.com, mhmandlu@ee.iitd.ac.in

***Abstract*—The key objective of this paper is to investigate a new biometric identifier for forensic and civilian applications. We propose a novel biometric authentication system based on low resolution finger nail plate images. Despite the uniqueness and high stability of the nail plate, its usage as a biometric identifier has not been extensively investigated for personal authentication. This paper implements a convenient and computationally efficient approach on low resolution nail plate images acquired with a contactless and unconstrained imaging setup. It exploits the local shape and texture of the nail plate by employing appearance based and texture based feature descriptors. Score-level fusion rules are utilized for integrating the nail plates from mainly three fingers of the hand. Extensive experimentation in both the biometric verification and recognition scenarios is carried out and the results validate the finger nail plates as a potential biometric identifier.**

Keywords- Biometric Authentication, Finer Nail plate surface, Independent component analysis, and Haar wavelet.

I. INTRODUCTION

Automated personal authentication using biometric technology is increasingly getting popular for effective security control in various civilian applications. Many different aspects of human physiology and/or behavior have recently been suggested in the literature to develop a comprehensive, biometric based authentication system [1]-[2]. There are several factors that are needed to be assessed while determining the suitability of any biometric trait since its performance is constrained by the conditions imposed by various real time applications. Hence, continuous efforts are required to explore other biometric modalities based on more advanced human features [3]-[6] in order to fulfill the varying requirements of the security applications. Recently, hand based biometrics has received high user acceptance due to the highly distinct and informative anatomical features available from hand. The key objective of this paper is to introduce a new biometric modality that can be extracted from the human hand for their potential to support human authentication. In this context, this paper investigates the capabilities and performance of the finger nail plate as a novel biometric modality and a distinctive personal attribute for personal authentication task. The anatomy of finger nail suggests that the uniqueness of the finger nail plate is characterized by the high individuality of the dermal structure underneath the finger nail plate, known as nail bed [7]-[8]. However, instead of utilizing the internal part of the nail organ i.e. finger nail bed for human identification, this paper utilizes the outermost part of the nail organ i.e. finger nail plate which is much easier to capture in contrast to finger nail bed. The universality and utility of the features extracted from the finger nail plate deserves attention for its use in civilian and/or forensic applications.

There are several hand based biometric schemes in the literature that has attracted a lot of research attention and has reached a certain level of maturity. Features extracted from the palmer part of hand is supposed to have more informational details than that from the dorsal part and several unimodal/multimodal biometric systems have been attempted based on palm-print [9], fingerprint [10] and palm vein biometrics [11]. However, the palmer part of the hand is more susceptible to spoof attacks and impersonation as people unconsciously leave their palm/finger prints on the objects they touch. Therefore, biometric modalities from the dorsal part of the hand like finger knuckles [12], hand dorsal vein pattern [13] which are more difficult to forge, are gaining popularity. Owing to the recent trend of touch-less acquisition, they have less chances of imposter attack and being a non-active part of the hand there are less possibilities of information degradation as compared to the palmer part. Also, civilian applications require that the biometric trait must ensure high measurability and user acceptance. In this regard, finger nail plate available from dorsal part of the hand proves to be a potential biometric modality and a promising alternative for personal authentication.

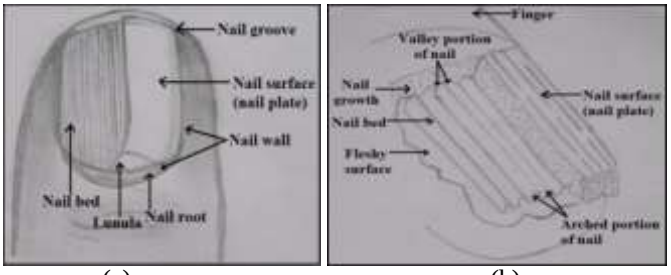

(a) (b)

Fig.1. Finger nail surface in (a), magnification of the nail bed structure in (b)

The cross section of the nail unit as in Fig. 1(a) is made of 3 tightly fused keratinized layers that are nail-plate, nail matrix and the nail-bed. The tongue-in-groove arrangement of the dermis and epidermis layers of the nail bed as explained in [7], [14] is referred to as arched and valley portion in Fig. 1(b) and it forms a structure that is unique, closely parallel and irregularly spaced. This grooved spatial arrangement of the nail bed is observed on the upper (convex) nail plate surface as longitudinal ridges/striations [14]. These longitudinal striations imitated on the nail plate surface are highly unique for every individual and serves as a means of personal authentication. Thus, the individuality in the uniqueness of nail plate based biometrics is completely dependent on the intrinsic anatomic characteristics of the nail organ.

A. The Motivation

The study of nail anatomy reveals that only the nail plate is regenerated as new cells are made, the spacing between the grooves of the nail bed remains constant over the entire life of the individual [15]. Thus, unlike face characteristics which changes with the age of an individual, the characteristics of the nail bed imitated on the nail plate can be very useful for identification over the entire lifespan of an individual. The works in [16], [17] illustrates that the presence of different keratin types in the layers of the nail organ is responsible for the variable physical characteristics of the individuals nail plate. Thus, the finger nail ridge patterns appearing on the nail plate surface shows a high degree of distinctiveness, even in the case of identical twins [18] or even between different finger nail plates of an individual. Moreover, the nail plate ridge pattern is in some way superior to other biometric traits for identification as the hardened nail structure resists any environmental effects, barring the changes caused by nail diseases/disorders and malnutrition [15], [19]. Onychomychosis [20], Psoriasis and Beau's lines are some of the diseases that affect the nail plate leading to its deformation in some way.

The key factor that is cited for the preference of nail plate based biometrics is that nail plate utilizes intrinsic characteristics of the nail bed for identification which is a hidden structure and hence crucial identity information is unrevealed. The nail plate is also an important substrate for diagnosis in field of forensic science [21]. However, forensically finger nails are not likely to be as useful as fingerprints for identification. Nevertheless, in a number of criminal cases broken finger nail plates have proved to be important in associating a suspect with the victim by comparing the nail ridge pattern [16].

B. Related Work

Despite of the uniqueness and high stability of the nail plate as a biometric modality, the use of nail plate surface as a means of personal authentication has not been extensively investigated in the literature. A US based company [22] is working on a technology that measures the narrowly spaced ridges and valleys on the nail bed using a laser. Their method utilizes a broadband interferometer technique to detect polarized phase changes in back-scattered light introduced through the nail plate and the ridged structure of the nail bed layer. By measuring the phase of the maximum amplitude signal, nail bed pattern is reconstructed using a pattern recognition algorithm. However, the technique employed in their work is inefficient for real time applications as it captures the detail of an internal part of the nail organ. Moreover, till now there has been a little development by the company in developing a prototype product and also no potential work has been published so far. The work by Apolinar and Rowe in [23], also examined the ridge pattern on the nail by means of a polarized light. They showed that the nail specimen display sharp bands of interference colors when it is oriented such that the direction of nail ridges is 45 deg from the direction of polarising filter. Their approach is however constrained as it restricts the movement of the finger nails during imaging. The work presented by the authors in [23] also requires a specially prepared thin nail specimen and hence the technique is not effective for civilian applications. Topping et al. [24] presented a system to measure the spacing of the capillary loops separated by valleys through the use of highly monochromatic light. The authors suggest significant improvements in the performance of nail recognition using such system, but the method and acquisition system they presented for nail identification involves a lot of computational complexity similar to the work in [22].

The prior research has made an attempt by analyzing the capability of finger nail as a biometric trait, but they lack an experimental analysis on a large public database so as to ascertain the statistical significance of their proposed approaches and also to generate a reliable conclusion on the potential of finger nail as a biometric identifier. *More importantly, till now there is no publically available finger nail database that researchers can utilize for comparison and benchmarking.* In addition, none of the work in [22]-[24] has shown any attempt to utilize the unique shape and texture characteristics of the nail plate to systematically compare the suitability of different feature representation techniques on finger nail plates.

C. Our Study

The review of research work in the past literature suggests that no proposal has been made to develop a completely automated user authentication system that utilizes low resolution (webcam) nail plate images. Our earlier work [25] on nail plate surface was the first attempt to investigate the possibility of utilizing the outermost part of the nail unit that is nail plate as a biometric modality. However, the results presented in [25] were in preliminary stages just to validate the potential of this new emerging modality.

This paper further explores the capabilities of nail plate based authentication for real world applications by employing various matching score integration strategies that ascertains the best possible performance. The main contributions from this paper can be summarized as follows:

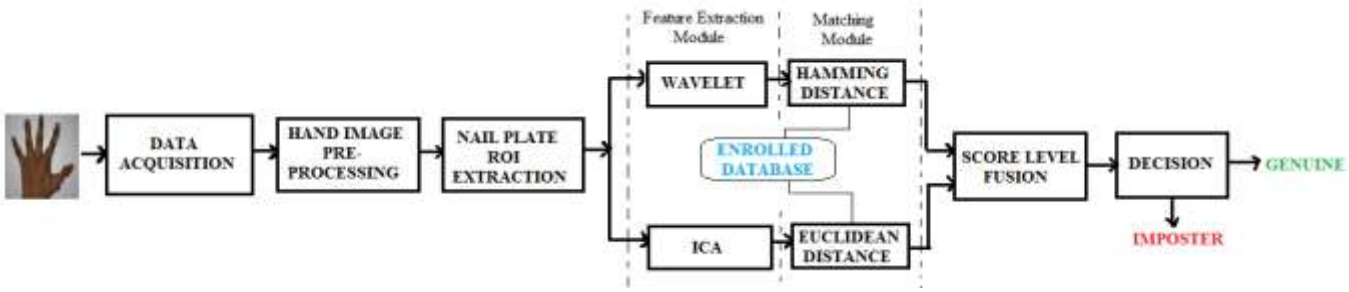

Fig.2. Block diagram of personal identification using nail plate surface

First, a completely automated and unified approach that utilizes a quite challenging and less researched finger nail plate images is presented for personal authentication. We have collected a large database of 900 hand samples from 180 users (5 samples per user) and has further segmented the nail plate regions of mainly index, middle and ring finger for feature extraction and matching. The outcomes of the rigorous experimental analysis carried out on 2700 nail plate images (180×5×3) suggest that the nail plate regions can prove to be a highly promising and novel biometric modality. Another related contribution of this paper is the use of peg-free and user friendly unconstrained imaging setup. This leads to a lot of inter and intra class variations, hence the steps for hand normalization and rotational alignment are proposed that effectively minimize any kind of resulting variations in the hand images. A robust scheme of global hand registration is proposed to normalize the hand images that further help to extract a rotation and translation invariant nail plate as region of interest (ROI).

Second, the nail plate surface segmentation approach presented in the paper is more refined than that presented in our earlier work in [25] and has the ability to accurately segment the ROI irrespective of the grown nail plate or presence of polishes over the nail plate surfaces (usually in case of female samples). The proposed approach for segmentation works at pixel level, by classifying each pixel into nail plate or non-nail plate region and then Gabor filtering technique is implemented that helps in completely automated and accurate extraction of nail plate ROI.

Third, rigorous experimental analysis is performed by employing various approaches for fusion of matching scores. The performance outcome from 2700 nail plate images ascertain the capabilities of finger nail plate as a promising biometric identifier and also validate the contributions from this paper. The rest of the paper is organized as follows: Section II presents the details on our unconstrained imaging setup and the block diagram in fig. 2 briefly explains the steps followed for developing a fully automated nail plate biometric system. Section III details the pre-processing steps applied on the acquired hand dorsal images, which includes hand segmentation, localizing hand extremities, global hand registration, finger decomposition and alignment. The approach followed for segmenting nail plate region from index, middle and ring finger is explained in Section IV. Section V gives the details on the feature descriptor that is Haar wavelet and Independent Component Analysis (ICA) that are utilized in our work for extracting salient nail plate features. The employed feature representation techniques provide the information about the shape and texture of the nail plate images. Section VI illustrates the various matching strategies followed in our work and also the rigorous experimental analysis carried out on the generated IIT Delhi nail plate database. The key conclusions from this work and the future scope of research on nail plate as a biometric modality is summarized in section VII.

II. Block Diagram and Imaging Set-up

The block diagram of the proposed system for biometric authentication is shown in fig. 2. Fig. 3(a) presents the acquisition system similar to that utilized in [25] for hand dorsal surface imaging. The images are taken from a Cannon A630 Digital Camera maintaining a resolution of 1600×1200 against a white background under uniform illumination. The imaging setup does not use any pegs or finger docking frame and user has the freedom of placing the hand in any orientation. Thus, the acquired hand images (see fig. 3(b)-(c)) present a lot of translational and rotational variations.

(a) (b) (c)

Fig.3. Unconstrained hand acquisition setup using webcam imaging in (a), acquired hand dorsal images in (b)-(c)

In order to extract a stable and aligned ROI, more stringent pre-processing steps are required which could register each finger by separate rotations to standard orientations as well as perform the rotation and translation of the whole hand. Finally, the normalized nail plate ROI are segmented from the three fingers and feature extraction algorithms are applied on them. The generated matching scores are then fused at score level by applying various techniques as in [26].

III. HAND IMAGE PREPROCESSING

In order to attain reliable and correctly aligned nail plate images as region of interest, the hand dorsum images are first subjected to preprocessing steps that include: 1) hand localization, 2) locating key points in the hand image, 3) global hand registration to accommodate rotation and

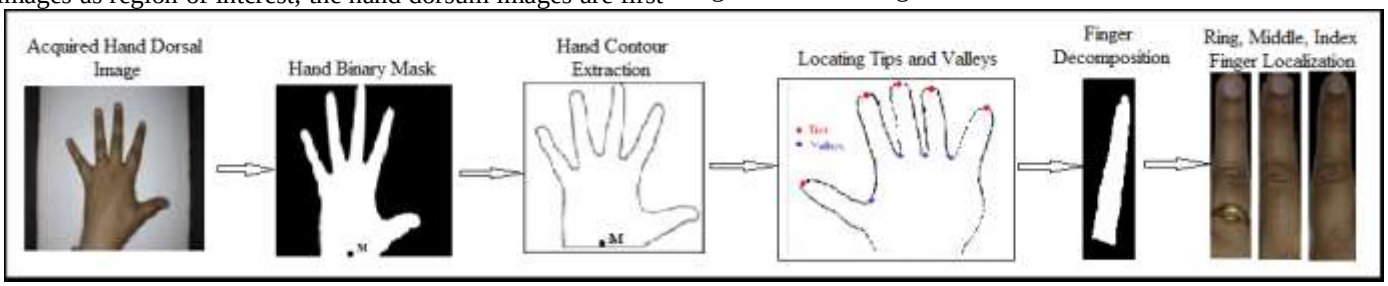

Fig.4. Block diagram to illustrate pre-processing steps followed for coarse finger localization and orientation

and translation variations, 4) finger decomposition. The block diagram shown in Fig. 4 briefly explains the various stages leading to localization of index, middle, ring finger. Each of the acquired hand dorsum image is first subjected to segmentation by subjecting them to a threshold operation. The pre-processing steps followed for hand localization are similar to that explained in [25]. The resulting binary mask in Fig. 4 is generated from the hand dorsum part which is further used for coarse finger localization and alignment.

A. Localization of Hand Extremities:

In order to eliminate the effect of rotation and translation variations, key points in the hand (finger tips and valleys) are located. The boundary pixels of the hand are traced from the binary hand mask and are stored in a boundary vector C_V. The key purpose of hand contour extraction shown in Fig. 4 is to locate local minima and local maxima points on the hand dorsum and to ensure that rotational alignment of the finger is carried out more precisely. The radial distances between the points in vector C_V and M that is midpoint of the hand wrist are computed and stored in a distance vector D_V. This approach is similar to the one employed in [12]. However, differing from their approach, this paper suggests a two moving window scheme to locate tips and valleys as maxima and minima on the distance signal. *W1* and *W2* represents the size of two windows used to locate the extremities along the distance distribution function, where *W1~N/20*, *W2~N/40* and N is the number of pixels in the hand contour. T and V represent the vector storing the tips and valley indices respectively found on the hand contour. The algorithm for locating hand extremities is as follows:

Function Find Extremities (W1,W2, D_V ,N,T,V)

While $k < N-W$
Increment the value of k by 1
window1 = $D_V(k, k+1,..., k+(W1-1))$
$i1$=min (window1)
$i2$=max (window1)

If $i2 \neq 1$ & $i2 \neq$ W1
If $(i2+ k-1 + W2) \leq N$ & $(i2+ k-1+W2) \geq 1$ **then**

window2 = $D_V(i2+ k-1-W2 ,..., i2+ k - 1 + W2)$
else if $(i2+ k - 1 - W2) < 1$ **then**
window2 = $D_V(1, 2,..., i2+ k - 1 + W2)$
else

window2 = $D_V(i2+ k -1 - W2, ... , N)$
end
$i3$= max (window2)
If $i3= W2 + 1$ **then**
Tip = $i2 + k-1$
Update $\boldsymbol{T}$ with the index of the found Tip
end
(Similarly, replace $i2$ with $i1$ and $i3$ with $i4$ where,
$i4$ = min (window2) to find Valley=$i1+k-1$ and
update V with the index of found Valley)
end
k = max (Tip, Valley, k)
end

B. Global Hand Registration

Once all the hand extremities on the radial distance function are located, the co-ordinate information of the hand is determined so as to perform hand normalization. The orientation of the palm is found with the orientation of its left and right edges. The palm edge E_{LF} at the side of little finger can be obtained by calculating the reference distance D_{ref}, which is fixed to 0.7 times of the distance from the tip of the little finger to the valley between ring and little finger for best outcome. The other index of the little finger valley, L_2 is incremented until the Euclidean distance between L_1 and L_2 is greater than D_{ref} where L_1 is the index of the valley between ring and little finger and L_2 is the other index of the little finger (see Fig. 5). A circle with L_2 as the centre, the edge segment of the hand contour lying within this circle is set as the palm edge E_{LF} at the side of little finger. The length L_M of the middle finger is determined as the distance measured from its tip to the mean of its surrounding valleys. A horizontal width vector H_{WV} is determined from the Eigen vector of the inertia matrix [27] extracted from edge E_{LF} and is taken orthogonal to its orientation. The palm edge E_{TIF} between thumb and index finger is extracted as the contour segment C lying between those of thumb and index fingers. The palm width W_P is given as:

$$W_P = (\text{mean of } E_{LF} - \text{mean of } E_{TIF}) \times H_{WV} \qquad (1)$$

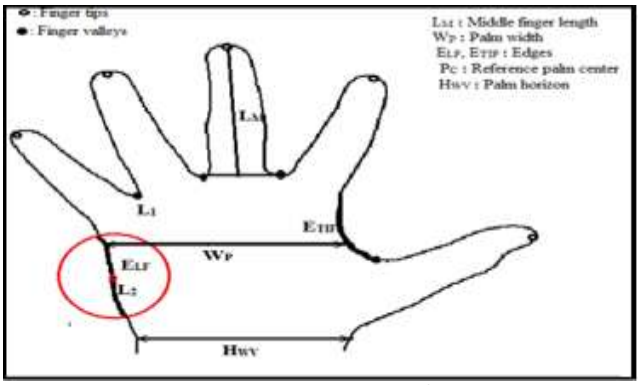

Fig.5. Diagram showing hand information

The global hand registration involves rotation and translation of the binary hand along the direction of the largest Eigen vector of the inertia matrix. The rotation angle Θ of the palm is found from its horizontal width vector H_{WV} which is a 2×1 matrix. It rotates the hand in the direction of the largest Eigen vector of the inertia matrix obtained from the palm edge at the side of little finger E_{LF}.

$$\Theta = sign \times \Re(\cos^{-1}([0\ -1] \times H_{WV})) \quad (2)$$

where, *sign* is the sign of the first element of H_{WV} which determines clockwise or counter clockwise direction of palm rotation and ℜ is the real part of the cosine inverse. Coarse localization of the finger pivots, that are joints somewhat below the line joining the inter finger valley, is performed by rotating them in the direction of the angle Θ, that is multiplying the finger pivots by the rotation matrix R and then translating the rotated finger pivots such that centroid coincides with the center of the image.

C. *Finger Decomposition*

Fingers are segmented by drawing a binary line of zeros between two adjacent valley points and applying connected component algorithm [28]. The initial alignment vector of each finger is found by fitting lines to a pair of contour segments found at either sides of the finger. These segments are extracted as the portion of finger contour lying between two concentric circles, with finger tip as the common centre. Finger's reference centre is found as the centroid of the portion of its shape image lying again between these circles. The extraction operation is however somewhat different for thumb. Re-orientation of each finger individually along the standardized direction without causing any shape distortions is achieved by determining the angle of the slope of the finger [29] and rotating it in counter clockwise direction. The mid-point of the finger (*x1*,*y1*) and its tip (*x2*,*y2*) gives the slope of each finger. The block diagram in Fig. 4 shows the localization of index, middle and ring finger along standard direction irrespective of hand position.

IV. NAIL PLATE SEGMENTATION

Once fingers are decomposed from the hand, nail plate region has to be segmented as ROI. It is to be noted that the segmented fingers are of varying size and thus a fixed nail plate ROI has to be extracted from them. Fig. 6 shows the block diagram of the proposed nail plate segmentation approach. Two approaches were investigated for nail surface extraction.

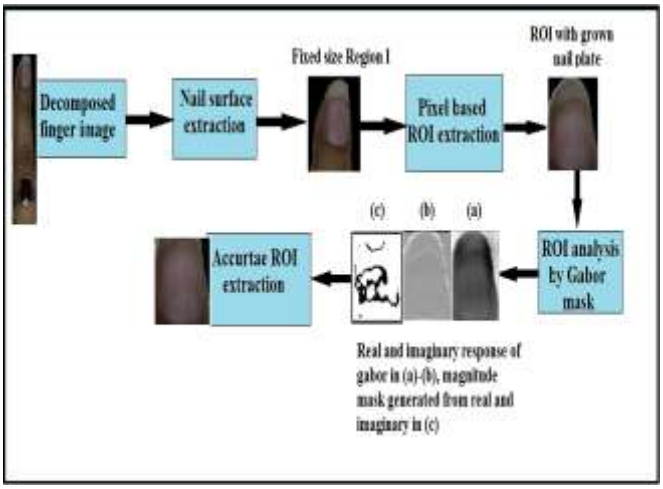

Fig.6. Block diagram of the proposed nail plate surface (ROI) extraction method.

Method 1: This approach extracts a fixed region of 100 pixels along the length of the three fingers, starting from the tip of the finger. However, it does not result in an accurate nail plate ROI segmentation, as a part of the skin following the nail (called as nail root) is also simultaneously extracted with the ROI in most of the cases, we name this extracted region as region-I (see fig 6). Another method is therefore investigated to further improve the localization of the ROI.

Method 2: The segmentation approach as explained in our earlier work in [25] adopts a pixel-based strategy to classify each pixel based on its gray level value. The pixel based segmentation approach discussed in [25] is still not accurate for samples with grown nail plate, as the grown part of the nail plate is also extracted along with the nail surface (see Fig. 6). In this paper we systematically develop a new approach for the nail plate segmentation using 2D Gabor filter. In order to minimize segmentation error for such cases the extracted ROI is processed by subjecting them to Gabor filter. The Gabor filters are known to achieve the maximum possible joint resolution in spatial and spatial-frequency domain and have been effectively utilized by researchers to develop texture and object segmentation paradigm [30].

The frequency and orientation selective characteristic of Gabor function is utilized to segment the part of the nail surface which has irregular textures due to the underlying nail bed structure from the part of the grown nail plate which shows no useful texture information. The Gabor function can be viewed as:

$$g(x,y,\theta,\mu,\sigma) = \frac{1}{2\pi\sigma^2}\exp\left\{-\frac{x^2+y^2}{2\sigma^2}\right\} \times \exp\left\{2\pi i\left(\mu x\cos\theta - \mu y\sin\theta\right)\right\} \quad (3)$$

where, μ is the frequency of the sinusoidal wave, Θ controls the orientation of the function, and $\boldsymbol{\sigma}$ is the standard deviation of the Gaussian envelope. Image analysis by Gabor mask generated from the real and imaginary part of the above function as in Fig. 6, identifies the location of non-nail surface pixels and hence we can easily segment the

nail surface images from the grown nail plate which contains redundant information. Optimized results are obtained by selecting Θ=0, μ=0.0916, $\boldsymbol{\sigma}$ =5.6179.

Fig.7. shows the automated extraction of nail plate surface of index, middle and ring fingers obtained from hand samples of the employed database.

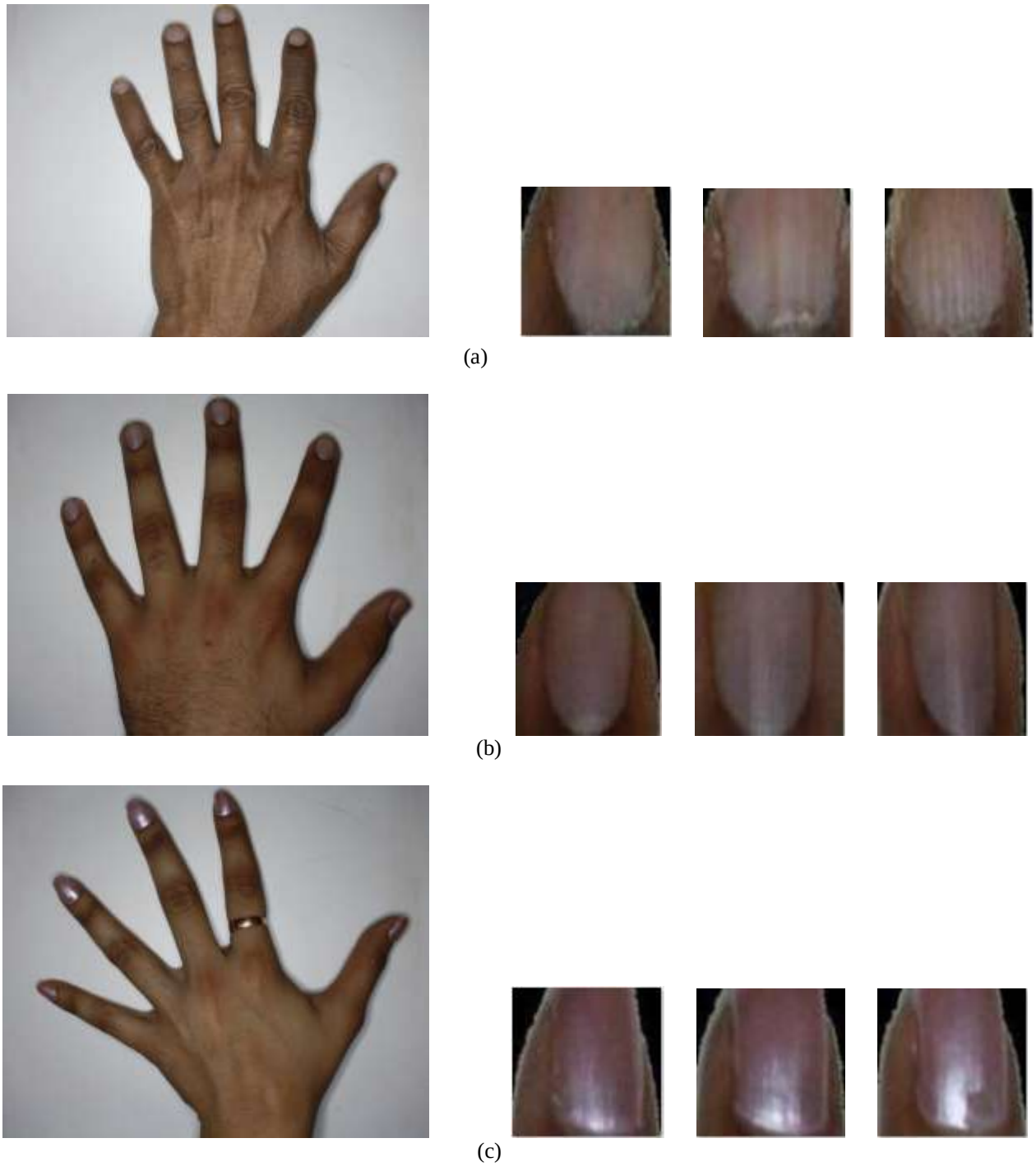

(a) (b) (c)

Fig. 7: Extracted nail plate surface region of index, middle, ring finger from acquired hand images in (a)-(c)

V. FEATURE EXTRACTION

There are several approaches that can be used for extracting reliable features which discriminates between nail plates of various users in a biometric application. The representation scheme proposed in this paper mainly extracts texture features and appearance based features that give information about the local shape and texture of the nail plate regions. The high individuality of the nail plate surface is mainly due to the random texture that is longitudinal striations observed over it and due to the distinct contour of the nail boundary. Hence, appearance and texture based feature descriptor used in this paper helps in extracting localized information that offer promising results for discriminating each individuals nail plate surface. We therefore investigated two such

promising approaches for generating matching scores from the nail plate images.

*A. **Haar Wavelet:***

The Haar wavelet [31]-[32] is the simplest possible wavelet, which can provide the information at the finest resolution of an image by forming a Haar wavelet pyramid. Thus it is able to detect global as well as local texture variations. It is a discontinuous step function and hence can be advantageous in analyses of images with spatial discontinuity. The mother wavelet ψ(t) of Haar wavelet can be defined as:

$$\psi(t)=\begin{cases}1, & 0\le t<\frac{1}{2}\\ -1, & \frac{1}{2}\le t<1\\ 0, & \text{otherwise}\end{cases} \quad (4)$$

and its scaling function can be defined as:

$$\varphi(t)=\begin{cases}1, & 0\le t<1\\ 0, & \text{otherwise}\end{cases} \quad (5)$$

The Haar wavelet pyramid is generated by applying the transform recursively to the low frequency approximation of the nail plate image obtained at each level which gives a series of detailed coefficients. The application of Haar wavelet on the original nail plate image of size 70×80 gives a Haar transformed image with approximation, diagonal, horizontal and vertical components as in Fig.9. In our approach Haar wavelets up to 5 levels are giving best results, as the higher levels gives much coarser information and lower levels gives much finer information thus losing the discrimination capability. The diagonal, horizontal and vertical coefficients of the 3rd, 4th and 5th level are found to have the most discriminative information and are employed to form a feature vector. The size of the feature vector is 3 times the size of the features of 3rd level (3×9×10), the features of the 4th level (3×5×5), and 3 times the features of the 5th level (3×3×3). Thus, a (1× 372) feature vector database is generated and each of its value is quantized to binary level by encoding positive value to 1 and negative value to 0.

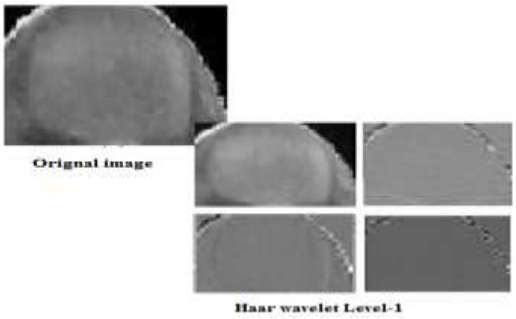

Fig. 8: Level-1 Haar transformation of the original nail surface

The binarized feature vector extracted from each of the finger nail plate image is then subjected to matching strategy to ascertain the degree of similarity between the two nail plate templates. Hamming distance [33] is used to determine the degree of similarity or dissimilarity and generates genuine and imposter matching score.

*B. **Independent Component Analysis***

The texture based feature descriptors based on Haar Wavelets described earlier in this section are not efficient in extracting useful information when the user nail plate surfaces are covered with nail polishes. For such cases, appearance based feature descriptors like Independent Component Analysis (ICA) are implemented on the nail plate images to extract texture plus local nail contour information.

The acquired images usually contain redundant information. As, detailed in [34] such redundancy can be exploited to organize into factor representation. In such representations, the dependencies among image pixels can be separated as independent components and used as appearance features. ICA is the computational method for separating a mixed signal into additive subcomponents of the non Gaussian signals [8]. ICA model represents the input source images $\{x_i(j), j=1,2,..K\}$ as a mixture of C unknown independent components rendered by an unknown mixing matrix M. Let the input image matrix be denoted as $X_{N\times K}$ where the columns K correspond to the lexicographically ordered images (for example- K=6400, if we have images of size 80×80) and rows N corresponds to the number of nail images. The detail of ICA feature extraction is now in order:

The ICA model considers a nail image as a combination of independent components (ICs) and a mixing matrix. Let $M_{N\times N}$ be the mixing matrix and $C_{K\times N}$ be the matrix of ICs for the data matrix $X_{K\times N}$. Then these matrices bear a relation:

$$X_{K\times N} = C_{K\times N} \times M_{N\times N} \quad (6)$$

The task in ICA is to estimate the independent components from the input image as:

$$C = X\times (M^{-1}) \quad (7)$$

Here, determining C from X is known as Blind Source Separation because the input source has to be separated into independent components without any knowledge of the mixing matrix. Though there are several approaches for the estimation of ICs from Eqn (7), we have considered the Fast ICA algorithm [35] that maximizes the statistical independence between the output components using maximization of the negentropy.

We have used here a nail-plate database of 180 users with 5 samples each. Each of the nail-plate images is of size 80×80. The mean-sample image for each user is computed by taking the average of 5 enrolled samples images. The mean-sample image is resized to get an image vector of size 6400×1. The mean-sample image is computed for all 180 users and the image matrix $X_{6400\times180}$ where K=6400 and N=180. As X is found to be of high dimensions, PCA is first employed on X for the dimensionality reduction. Let $U_{6400\times180}$ be the projection (Eigenvector) matrix and $Mean_{6400\times1}$ is the mean vector arising from the application of PCA on X. The image

matrix X is then transformed by PCA to get the projection matrix $Y_{180\times180}$ as follows:

$$Y_{150\times150}=(X_{22500\times150})^{T}\times U_{22500\times150} \quad (8)$$

By applying the Fast ICA algorithm on projected matrix Y we obtain the IC matrix $C_{180\times180}$ using Equations (6) and (7). At the verification/identification stages, let $Q_{6400\times1}$ be the image matrix computed from input hand-shape image. Subtracting the mean vector $Mean_{6400\times1}$ from it leads to

$$Vector1_{6400\times1}= Q_{6400\times1} - Mean_{6400\times1} \quad (9)$$

Multiplying the Vector1 with the PCA projection matrix gives the Eigen feature vector as:

$$Eigenfeature_{1\times180}= Vector1_{6400\times1}^{T} \times U_{6400\times180} \quad (10)$$

Use of the IC matrix on the Eigen feature vector yields the ICA feature vector as:

$$ICAfeature_{150\times11} = B_{180\times180} \times Eigenfeature_{1}\times180^{T} \quad (11)$$

Here the Euclidean distance [36] is used to match two ICA feature vectors. Let $ICAV_1$ and $ICAV_2$ be the two ICA features computed using Eq. (8)-(11). The matching score between these two vectors using Euclidean distance is computed as:

$$s=\sqrt{\sum_{i=1}^{180}\{ICAV_1(i)-ICAV_2(i)\}^2} \quad (12)$$

VI. Experimental Overview and Results

The experiments are performed in mainly three phases to ascertain the usefulness of nail plate for biometric authentication. The database of 180 users for experimentation is collected at Biometrics Research Laboratory, IIT Delhi since to the best of our knowledge there is no publically available database on nail plate images. The dataset consists of 900 left hand sample images acquired from 180 users using the imaging set up detailed in section II. The 2700 nail plates of three fingers that is index, middle and ring are generated from these 900 hand samples for generating matching scores and performance analysis.

First, the robustness of Wavelet and ICA algorithm on individual finger nail plate surface that is index, middle and ring is evaluated. Each of the 180 users has provided 5

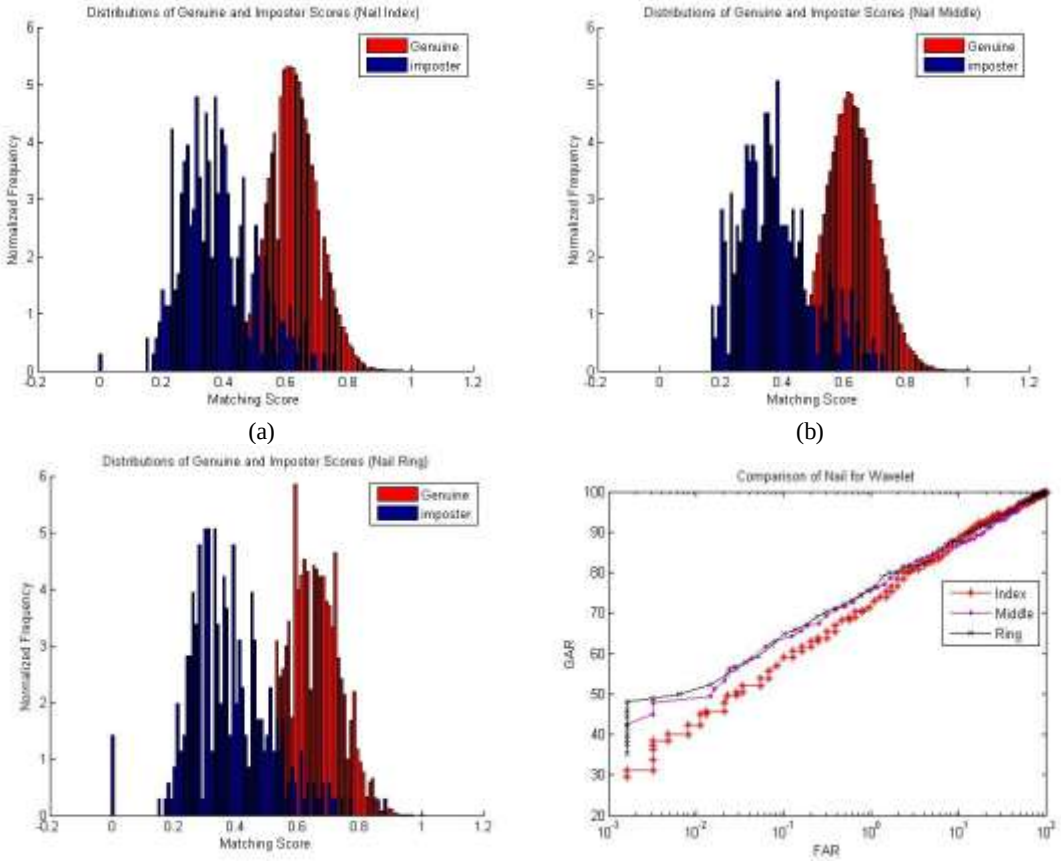

Fig.9. Genuine and impostor distribution for Wavelet (a) index (b) middle and (c) ring (d) their combined ROC.

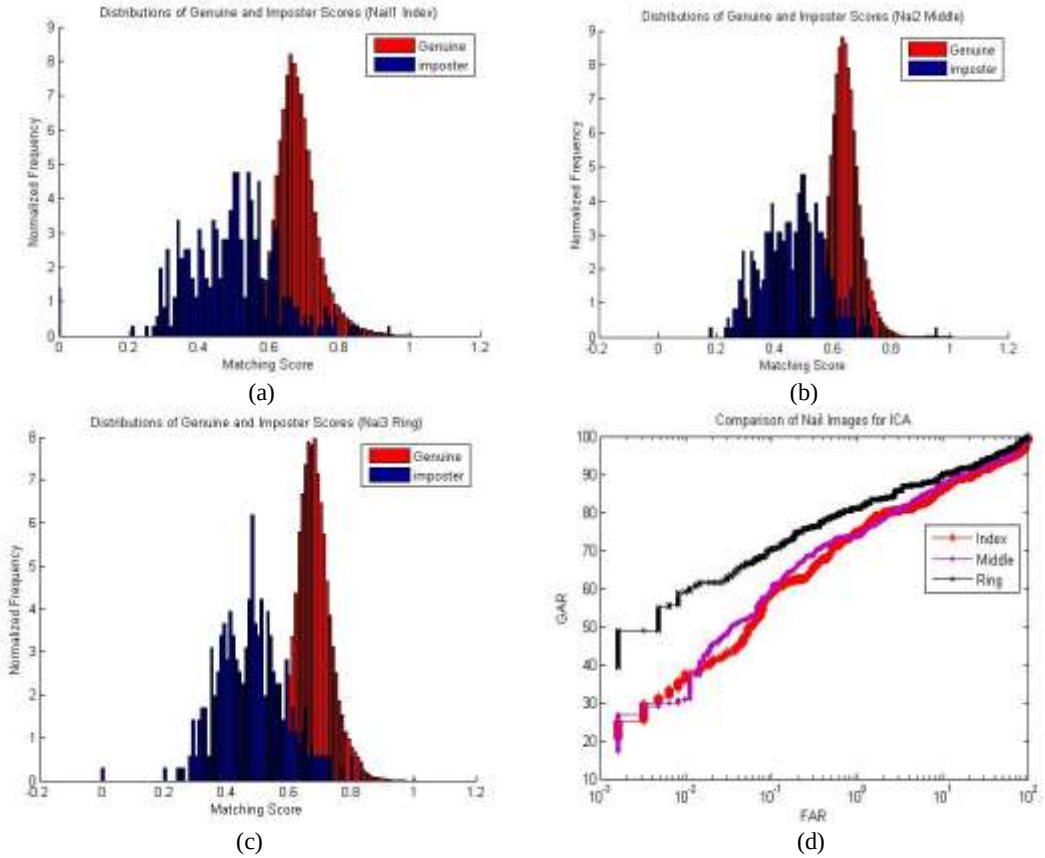

Fig.10. Genuine and impostor distribution for ICA (a) index (b) middle and (c) ring (d) their combined ROC.

images, out of which 3 images per user are considered for training and 2 images per user for testing purpose. Therefore, the number of genuine matching score are 360 (180 × 2) and imposter matching score are 64440 (180 × 179 × 2) for each of the three nail plate regions. The distribution of genuine and imposter matching scores for the 3 nail plate surface generated from Wavelet is illustrated in fig. 9(a)-(c). ROC curve (plot of GAR Vs FAR) for these finger nail-plate surfaces corresponding to wavelet feature is shown in Fig. 9 (d). Ring finger nail plate surface yields best performance among the 3 nail plate surfaces with GAR= 50% at FAR= 0.001% and GAR=76% at FAR=1%.

The distribution of genuine and imposter matching scores for the 3 nail plate surface generated from ICA is illustrated in Fig. 10 (a)-(c). ROC curve for the three finger nail-plate surfaces corresponding to ICA feature is shown in Fig. 10 (d). Similar to the results in Fig. 9 (d), Fig. 10 (d) also shows that the ring nail plate surface yields best performance among the three nail plate regions with GAR=50% at FAR=0.001%. However, the performance comparison of ring finger nail plate surface for both the representation technique at FAR=1% as shown in Fig. 11 informs that ICA operate on better performance (GAR=80%) than wavelet features (GAR=76%).

In the second set of experiment, the multiple observations from 3 nail plates are effectively integrated for performance improvement. The multiple observations can be fused at various levels: fusion before matching (feature extraction level) and fusion after matching (match score, rank, decision). In this paper, we perform score level combination as it is expected to give better performance and has been extensively studied in the literature [4].We utilize two score level fusion schemes that is sum and product [20] for fusion of ring finger nail plate surface features obtained from ICA and wavelet. The performance of the two fusion rules in Fig. 12 (a) shows that product rule gives the best result (GAR=85%) while sum rule yield result similar to ICA (GAR=80%) at FAR=1%.

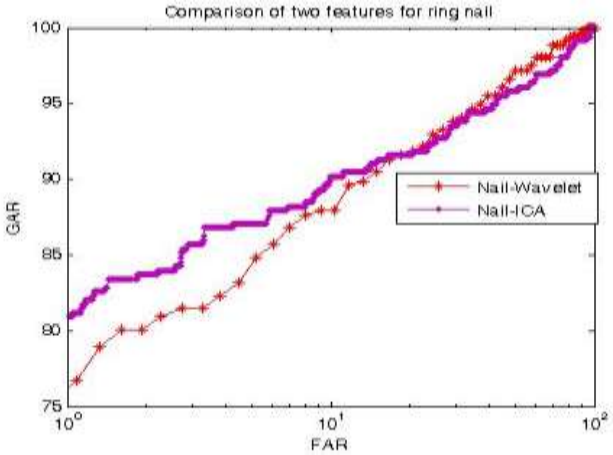

Fig.11. Comparison of ICA and Wavelet Features

Now, product rule is used to fuse all the three (ring, middle, and index) finger nail-plates corresponding to each Wavelet and ICA algorithm separately. The fused matching

scores of nail plate surface features from ICA and Wavelet are further fused using the same product rule as shown in Fig. 12(b)-(c). Fig. 12(b) shows the GAR on fusion of three nail images (ring, middle, and index) for ICA (GAR=90%), Wavelet (GAR=87%), and their fusion (GAR=93%, product rule) at FAR=1%. Fig. 13 (c) shows a trade-off between two error rates by displaying lowest possible FAR=0.001% and the corresponding GAR for ICA (GAR=85%), wavelet (GAR=76%), and their product (GAR=61%). In both the cases, it can be observed that the fusion of the two features yields the better performance as compared to individual features extracted from the nail plate surfaces. The selection of an appropriate FAR and GAR is application dependent [26].

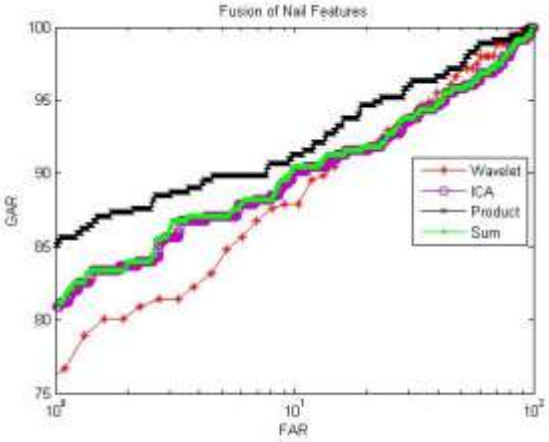

(a)

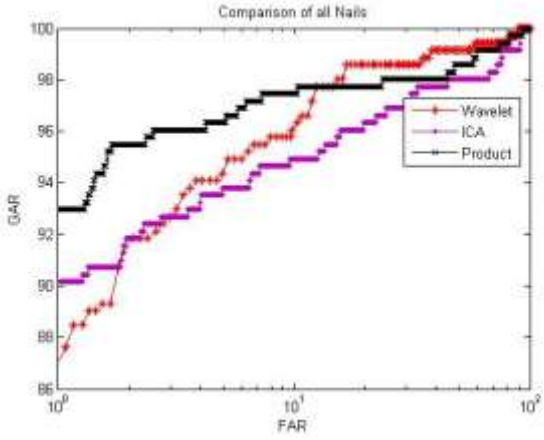

(b)

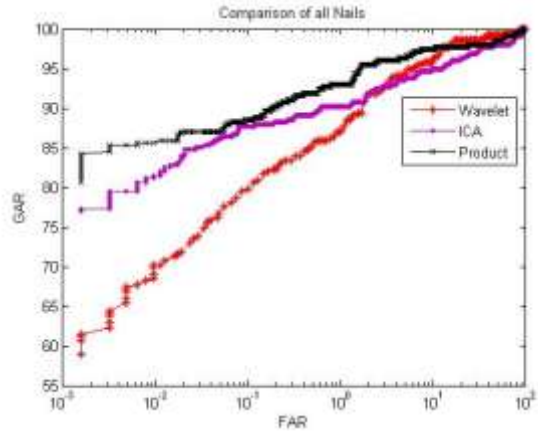

(c)

Fig.12. Wavelet and ICA fusion: for ring finger nail plate using sum and product rules in (a); A trade-off between error rates for all 3 nail plates: at FAR=1% in (b) and FAR=0.001% in (c)

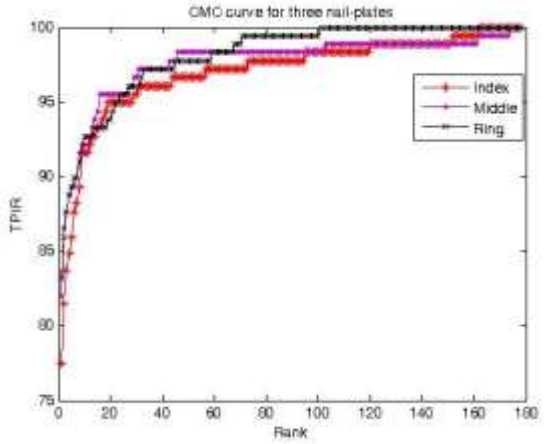

(a)

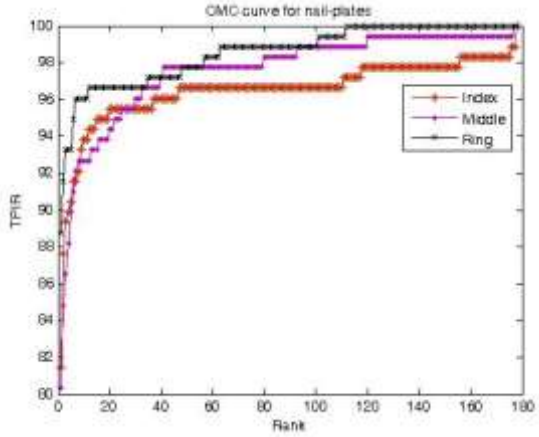

(b)

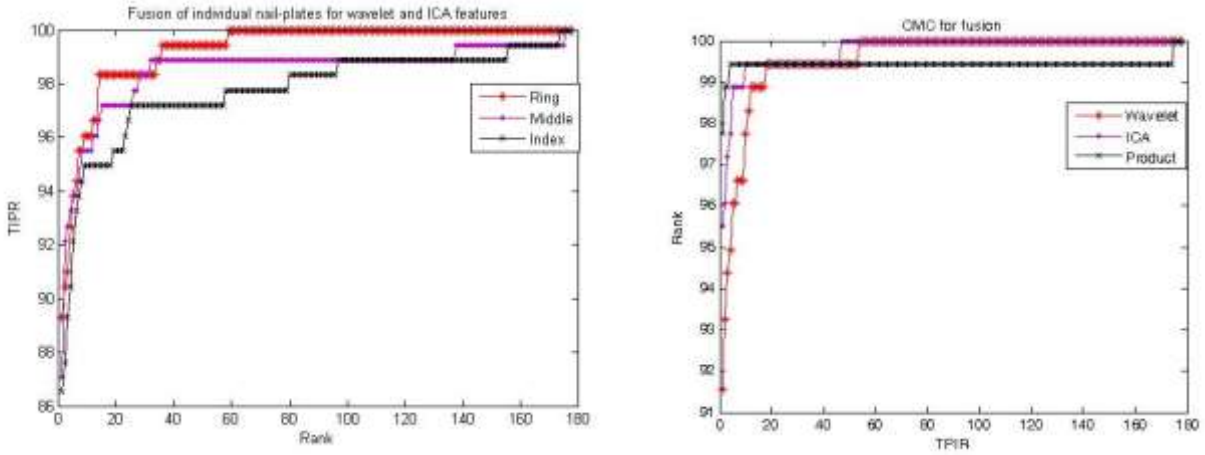

(c) (d)

Fig.13. CMC curve for 3 nail-plate surfaces: for Wavelet features in (a); for ICA features in (b) CMC for fusion of: individual nail-plates for wavelet and ICA in (c);all 3 nail plates for the 2 features in (d)

Table1: TIPR (%) rates for three nail-plates individual and their fusion at rank-1 recognition

	Wavelet	ICA	Fusion
Ring	83	89	89.5
Middle	82	80	86.5
Index	76	81	87
Fusion	**91.5**	**96.5**	**98**

In the third set, the experimental results for recognition/identification performance using nail plate features are reported. We have computed CMC for each of the ring, middle, and index finger nail-plate as shown in Fig. 13(a), which shows that that ring finger nail plate surface yields best recognition rate (83%) at rank-1 recognition in comparison to middle (82%) and index (76%) fingers nail plate surfaces. The CMC for the score-level fusion of ICA and wavelet features shown in Fig. 13 (b) also confirms the best rank-1 recognition result of ring finger nail plate with ring (89%), middle (80%), and index (81%). The CMC for fusion of individual nail-plate surfaces for ICA and Wavelet features is shown in fig. 13(c), while CMC for integration of all three nail-plates for

Wavelet, ICA, and their fusion using product rule is shown in Fig. 13(d). It can be noted that, the fusion of three nail-plates for ICA and Wavelet operate on rank-1 recognition rates of 91.5% and 96.5% respectively while their product yields the best recognition performance of 98%. The true identification rates for the nail-plate surfaces for rank-1 recognition are shown in Table 1.

VII. Discussion and Conclusion

This paper presents a novel and fully automatic nail plate based authentication system. The ridge pattern on the finger nail plate surface has high stability over entire lifetime and is highly unique for every individual. A survey of current biometric modalities shows that very less attempt has been made to investigate the capability of the nail plate as a biometric identifier. However, the rigorous experimentation performed in 3 phases on a database of 180 users with 5 samples of each user and three nail (ring, middle, and index finger) plate surface of each samples, hence 2700 (180×5×3) nail-plate images shows the potential and individuality of this new biometric identifier which can be applicable in several medical, surveillance, and forensic applications in the near future of biometrics.

The score level fusion techniques applied on genuine and imposter matching scores from three nail plate regions of an individual (ring, middle and index) gives significant performance improvement compared to individual representation. The product rule is found to be the best performing rule with highest verification rates. We have also implemented recognition for all three nail-plates and their fusion using product rule. The recognition rates for the all the nail-plates are shown in Table 1.

To the best of our knowledge, there has been no work on user authentication using peg free, low resolution nail-plate images which also takes into consideration nail plate growth (see fig. 7) and the presence of nail paint over the nail plate and simultaneously provides a successful verification/recognition rate irrespective of these two factors. It can be possible that the appearance based features employed in this work may not work well for large scale population and some other more descriptive feature extraction algorithms are still required to be experimented. But our experimental results have suggested that the proposed approaches can certainly be useful for personal authentication in small and medium sized population. More importantly, high performance results using score level fusion rules achieved from low resolution image samples proves that such information can be highly useful when the quality of nail plate surface in an individual is weak or unstable. It can be noted that, the acquisition of whole dorsal part can be also utilized to segment other biometric modalities like finger knuckles [12], dorsal vein [13] for fusion with finger nail plates to develop a multimodal

system and is among one of the future works. Although a lot remains to be done, yet our results to date indicate that the proposed nail plate based features constitutes a promising addition to the biometrics-based personal authentication. The system configuration in this work is Core 2 Quad, 4 GB RAM, and the MATLAB 2010 without incorporating any optimization of the codes.

REFERENCES

[1] A. K. Jain, P. Flynn, and A. A. Ross , Handbook of biometrics. Springer, New York, 2007.

[2] R. Mandelbaum, "Vital Signs of Identity," *IEEE Spectrum*, pages 22-30, February 1994.

[3] Biometric Technology Today, vol. 12, issue 5, pp. 1-12, May 2004. Available-http://www.elsevier.com/journals/biometric-technology-today.

[4] G. Goudelis, A. Tefas, and I. Pitas, "Emerging biometric modalities: a survey," *J. Multimodal User Interfaces*,2008, pp. 217–235, Sept. 2009.

[5] A. K. Jain, A. Ross, and S. Pankanti, "An Introduction to biometric recognition," *IEEE Trans.Circuits & Sys. Video Tech.*, vol. 14, no. 1, pp. 4-20, 2004.

[6] K. Nandakumar, "Integration of multiple cues in biometric systems", *PhD thesis*, Department of Computer Science & Engineering, Michigan State University, East Lansing, USA, 2005.

[7] U. Runne, and C. E. Orfanos, 1981. The human nail – structure, growth and pathological changes. Curr. Probl. Dermatol. 9, pp.102–149.

[8] H. P. Baden, "The Physical Properties of Nail," *Journal of lnvestigative Dermatology*, vol. 55, no. 2, pp. 115-122, 1970.

[9] D. Zhang, W. K. Kong, J. You, and M. Wong, "Online palmprint identification," *IEEE Trans. Pattern Analysis and Machine Intelligence*, Vol. 25 (9), pp. 1041-1050, 2003.

[10] N. Ratha, and R. Bolle, Automatic Fingerprint Recognition Systems, Springer, 2004.

[11] J. G. Wang, W. Y. Yau, A. Suwandy, and E. Sung, "Person recognition by fusing palmprint and palm vein images based on "Lapacian palm" representation," *Pattern Recognition*, vol. 41, pp. 1531–1544, 2008.

[12] A. Kumar and Ch. Ravikanth, "Personal authentication using finger knuckle surface," *IEEE Trans. Info. Forensics & Security*, vol. 4, no. 1,pp. 98-110, Mar. 2009.

[13] M. Ramalho, P. L. Correia and L. D. Soares," Biometric identification through palm and dorsal hand vein pattern," *Eurocon International Conf on Comp. as a tool*, pp 1- 4, April 2011.

[14] R. V. Kristic, Human Microscopic Anatomy, Ed. New York: Springer-Verlag, 1991.

[15] A. A. Diaz, A. F. Boehm, and W. F. Rowe, "Comparison of Fingernail Ridge Patterns of Monozygotic Twins," *Journal of Forensic Sciences*, JFSCA, Vol. 35, No.1, pp 97-102 , Jan 1990.

[16] H. H. Bragulla, and D. G. Homberger," Structure and functions of keratin proteins in simple, stratified, keratinized and cornified epithelia," *J. Anat. 214*, pp. 516–559, 2009.

[17] L. N. Nieto, J. L. Gómez-Amoza, M. B. Delgado-Charro,and F. J. Otero-Espinar," Hydration and N-acetyl-l-cysteine alter the microstructure of the humannail and bovine hoof: implications for drug delivery," *J. Control. Rel. 156*, pp. 337–344, 2011

[18] C. Ralph III, B. M. Piraccini, and A. Tosti, "The nail and hair in forensic science," Journal of American Academy of Dermatology, Vol. 50, Issue 2, pp 258-261 , Feb 2004.

[19] J. R. K. Robson, Hardness of finger nails in well-nourished and malnourished populations. *Br. J. Nutr.*, vol. 32, pp. 389-394, 1974.

[20] W. D. Taylor, D. T. Roberts and J. Boyle, " Guidelines for treatment of Onychomychosis," British Journal of Dermatology, 148. 402-410, Oct. 2002.

[21] H. L. MacDonell and L. F. Bialousz, "Evaluation of Human Fingernails as a Means of Personal Identification," in *Legal Medicine Annual: 1972*, Cyril Weeht, Ed., Appleton-Century-Crofts, New York, 1972, pp. 135-143.

[22] Nail ID. BIOPTid the human barcode (2009). Biometrics systems division, Available: http://www.humanbarcode.com.

[23] E. Apolinar and W. F. Rowe, "Examination of Human Fingernail Ridges by means of polarized light," *Journal of Forensic Sciences*, JFSCA, Vol. 25, No. 1, pp. 154-161, Jan. 1980.

[24] A. Topping, V. Kuperschmidt, and A. Gormley,"Method and apparatus for the automated identification of individuals by the nail beds in their fingernails," U.S. Patent 538 641, Oct. 4, 1995.

[25] Shruti Garg, A. Kumar, M. Hanmandlu ,"Biometric authentication using finger nail surface," *International Conference on ISDA*, pp-497-502, Nov. 2012

[26] A. Ross, A. Jain, "Information Fusion in Biometrics", *Pattern Recognition Letters*, Vol. 24 pp. 2115–2125, 2003

[27] W. Spong, B. Srinivasan, F. Ghorbel, "On the uniform boundedness of the inertia matrix of serial robot manipulators, " *Journal of Robotic Systems*, Vol. 15, No. 1, Jan 1998.

[28] R. D. Yappa and K. Harada, "Connected component labelling algorithm for gray scale images and evaluation of performance using Digital Mammograms," *International journal of Comp.Sc and National Security*, vol.8, no.6, June 2008.

[29] Y. Zhou, A. Kumar, " Human identification using finger images," *IEEE trans on imag processing*, Vol. 21, pp. 2228-224, April 2012.

[30] D. M. Weber and D. Casasent, "Quadratic Gabor filters for object detection," *IEEE Trans.Image Process.*, vol. 10, pp.218-230, Feb. 2001.

[31] E. Stollnitz, T. DeRose, D. Salesin, Wavelet for Computer Graphics: Theory and Applications, Morgan Kaufmann, Los Altos, CA, 1996

[32] S. G. Mallat, "A theory for multiresolution signal decomposition : the wavelet representation," *IEEE Transactions on Pattern Analysis and Machine Intelligence*, vol. 11, pp. 674-693, 1989.

[33] W. Hamming, "Error detecting and error correcting codes," *Bell system Tech. Journal*, vol. 29, no. 2, pp. 147-160, 1950.

[34] M. S. Bartlett, J. R. Movellan, and T. J. Sejnowski, "Face Recognition by Independent Component Analysis", *IEEE Transactions on Neural Networks*, Vol. 13, No. 6, November 2002.

[35] A. Hyvarinen and E. Oja, "Independent component analysis: algorithms and applications," *Neural Netw.*, vol. 13, no. 4–5, pp. 411–430, 2000.

[36] Elena Deza & Michel Marie Deza, *Encyclopedia of Distances*, Springer, 2009.

Author Biographies

Shruti Garg received her B.Tech in Electronics and Communication Engineering from Gautam Budhh Technical University, Uttar Pradesh, India in 2010. She joined Department of Electrical Engineering, Indian Institute of Technology, Delhi, India in July 2011. She has since been working towards her Master of Science (Research) in the same department. Her research interests include image processing, pattern recognition with emphasis on personal authentication using biometric technologies.

Amioy Kumar received his M.Sc. degree from Department of Mathematics, Indian Institute of Technology Roorkee, India in 2006. He joined Biometrics Research Laboratory, Department of Electrical Engineering, Indian Institute of Technology, Delhi, India in November 2006 and has since been working towards his MS (Research) and then doctoral research (pursuing) in the same department. His research interests include pattern recognition with emphasis on biometric based personal authentication and multibiometric systems.

Madasu Hanmandlu received his B.Tech.(Power systems) from REC Warangal, Jawaharlal Nehru Technological University (JNTU), India, in1976, and Ph.D. (Control Systems) from Indian Institute of Technology (IIT), Delhi, India, in 1981. Presently working as a Professor in department of Electrical Engineering, IIT, Delhi. His current research interests mainly include: Fuzzy modelling for dynamic systems and applications of fuzzy logic to image processing, document processing, medical imaging, multimodal biometrics, surveillance and intelligent control. He has authored a book on Computer Graphics and published more than 250 publications in both conferences and journals. He has guided 18 PhDs and 100 M.Tech. students.